Solution Structure of the Second Extracellular Loop of Human Thromboxane A_2 Receptor†

Ke-He Ruan,* Shui-Ping So, Jiaxin Wu, Dawei Li,‡ Aimin Huang, and Jennifer Kung

Vascular Biology Research Center and Division of Hematology, Department of Internal Medicine, The University of Texas Health Science Center, Houston, Texas 77030

Received August 8, 2000; Revised Manuscript Received October 10, 2000

ABSTRACT: Thromboxane A_2 receptor (TP receptor), a prostanoid receptor, belongs to the G protein-coupled receptor family, composed of three intracellular loops and three extracellular loops connecting seven transmembrane helices. The highly conserved extracellular domains of the prostanoid receptors were found in the second extracellular loop (eLP_2), which was proposed to be involved in ligand recognition. The 3D structure of the eLP_2 would help to further explain the ligand binding mechanism. Analysis of the human TP receptor model generated from molecular modeling based on bacteriorhodopsin crystallographic structure indicated that about 12−14 Å separates the N- and C-termini of the extra- and intracellular loops. Synthetic loop peptides whose termini are constrained to this separation are presumably more likely to mimic the native loop structure than the corresponding loop region peptide with unrestricted ends. To test this new concept, a peptide corresponding to the eLP_2 (residues 173−193) of the TP receptor has been made with the N- and C-termini connected by a homocysteine disulfide bond. Through 2D nuclear magnetic resonance (NMR) experiments, complete ^{1}H NMR assignments, and structural construction, the overall 3D structure of the peptide was determined. The structure shows two β-turns at residues 180 and 185. The distance between the N- and C-termini of the peptide shown in the NMR structure is 14.2 Å, which matched the distance (14.5 Å) between the two transmembrane helices connecting the eLP_2 in the TP receptor model. This suggests that the approach using the constrained loop peptides greatly increases the likelihood of solving the whole 3D structures of the extra- and the intracellular domains of the TP receptor. This approach may also be useful in structural studies of the extramembrane loops of other G protein-coupled receptors.

Prostanoids, comprising prostaglandins and thromboxane, are a family of bioactive oxygenated metabolites of polyunsaturated fatty acids synthesized by vascular smooth muscle and endothelium (*1, 2*) in response to various physiological and pathological stimuli (*3*). Prostanoids act as local hormones in the vicinity of their production site to regulate hemostasis and smooth muscle functions, which are mediated by specific plasma membrane receptors. The receptors are classified into five basic types based on the sensitivity to prostaglandin D_2 (PGD_2), prostaglandin E_2 (PGE_2), prostaglandin F_2 (PGF_2), prostaglandin I_2 (PGI_2), and thromboxane A_2 (TXA_2), and are termed DP, EP, FP, IP, and TP receptor, respectively (*4*). In addition, EP receptors are subdivided into four subtypes, EP1, EP2, EP3, and EP4 receptors, based on the responses to various agonists and antagonists. Of the prostanoid receptors, human TP receptor was first purified from platelet in 1989, and the cDNA was cloned from placenta in 1991 (*5, 6*). Other human prostanoid receptor cDNAs have also been cloned by homology screening, and their primary molecular structures and biological functions were identified (*4*). All of the known prostanoid receptors belong to the rhodopsin-type G protein-coupled receptor superfamily, with seven hydrophobic transmembrane domains. The prostanoid receptors recognize ligand molecules on the extracellular side of the membrane and then interact with heterotrimeric G proteins on the intracellular side. The activated G protein subsequently initiates a second messenger system of intracellular signaling (*4*).

The cDNA for human TP receptor, cloned from placenta, encodes a protein of 343 amino acids (*6*). Recently, the cDNA for another TP receptor was isolated from human endothelial cell, which has a different C-terminal tail, resulting from alternative splicing (*7*). These receptors are the same with regard to signal transduction, but the endothelium expressed only the spliced form, and the placenta expressed both types of TP receptors (*3*).

The highly conserved regions of the prostanoid receptors were found in the second extracellular loop and the third and seventh transmembrane domains. These conserved regions are proposed to be involved in the contact with the common structures of the prostanoids which contain carboxylic acid, hydroxyl groups at position 15, and two aliphatic side chains (*3*).

† This work was supported by NIH Grants HL 56712 and NS 23327. The NMR facility at The University of Texas Health Science Center in Houston is funded by the W. M. Keck Foundation.

* To whom correspondence should be addressed at the Division of Hematology, Department of Internal Medicine, The University of Texas Health Science Center at Houston, 6431 Fannin St., Houston, TX 77030 (Tel: 713-500-6769; Fax: 713-500-6810; Email: kruan@imed2010.med.uth.tmc.edu).

‡ Current address: National Institutes of Health, Mail-Drop E3-01, National Institute of Environmental Health Science, Research Triangle Park, NC 27709.

10.1021/bi001867c CCC: $20.00
Published on Web 12/07/2000

Several recombinant human TP receptors with point mutations at W299R, W299L, R295Q, or L291F in the seventh transmembrane domain lost binding activity to SQ29,548, an antagonist of the receptor, and suggested that the transmembrane domain is involved in forming a ligand binding pocket (*8*). Both Dorn II's group and Tai's group demonstrated that TP receptors with point mutations at C102, C105, or C183 located in the first and second extracellular loops exhibited no ligand binding activity, suggesting that the residues in these two extracellular loops also contribute to proper ligand binding (*9, 10*). Using homology analysis, Tai further suggested that C102 in the first loop plays an essential role in ligand binding, and that C105 in the first loop and C183 in the second loop may form a disulfide bond to stabilize the receptor (*10*). In addition, a TP receptor mutant with S201A in the fifth transmembrane domain also lost ligand binding activity, suggesting that S201 may be involved in a polar interaction with TXA_2 (*10*). Chimeric receptor studies performed by both Dorn II's group and Narumiya's group also suggested that the multiple domains of the prostanoid receptors including TP, IP, and DP are involved in ligand recognition (*11, 12*). Recently, residues 198−205 in the second extracellular loop of the EP3 receptor have been identified as an essential determinant of ligand selectivity (*13*). The above results clearly support that the extracellular domains of prostanoid receptors are involved in ligand recognition. However, the segments and residues of the prostanoid receptors responsible for specific ligand recognition have not been thoroughly examined. Structural characterization of the extracellular functional domains of the TP receptor represents a key step in understanding the specificities in ligand recognition of the receptor. In this paper, an initial working model for the human TP receptor structure was constructed by molecular modeling based on the bacteriorhodopsin structure, and was used to guide our peptide design. The 3D structure of a constrained loop peptide mimicking the second extracellular domain of human TP receptor was solved by the high-resolution 2D[1] ^{1}H NMR technique. Results from the studies provide evidence to solve the 3D structures of these important domains of other prostanoid receptors and other G protein-coupled receptors in general.

MATERIALS AND METHODS

Materials. Trifluoroacetic acid (TFA) was obtained from Millipore (Bedford, MA). D_2O was from Cambridge Isotope Laboratories (Andover, MA). SQ29,548 was purchased from Cayman Chemical (Ann Arbor, MI).

Peptide Synthesis. A peptide mimicking human TP receptor eLP_2 (residues 173−193) with homocysteine added at both ends of the loop was synthesized using the fluorenylmethoxycarbonyl-polyamide solid phase method. After cleavage with TFA, the peptide was purified to homogeneity by HPLC on a Vydac C4 reversed phase column with a gradient from 0 to 80% acetonitrile in 0.1% TFA. For the cyclization of peptide by disulfide bound formation, purified peptide is dissolved in 1 mL of DMSO, and added to H_2O at a final concentration of 0.02 mg/mL. The solution is adjusted to pH 8.5 using triethylamine, and stirred overnight at room temperature. The cyclic peptide is then lyophilized and purified by HPLC on the C4 column. The sequence of the synthesized TP receptor eLP_2 peptide is shown in Figure 1.

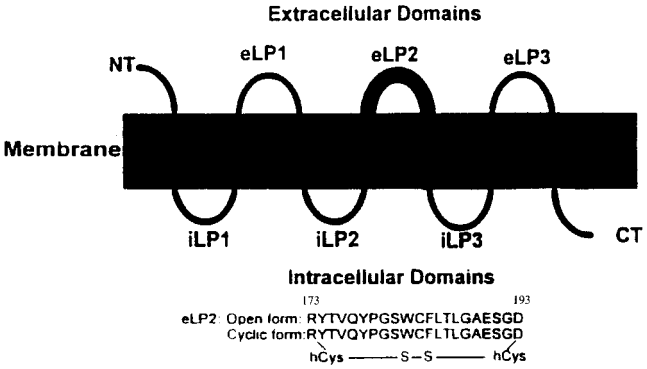

FIGURE 1: Topology model of the TP receptor. The heavy line (eLP2) represents the region for the studies. The amino acid sequence of the region synthesized is shown in the open form, and the constrained loop form which has a connection between the N- and C-termini by a disulfide bond using additional homocysteine (hCys) residues. eLP: extracellular loop. iLP: intracellular loop. CT: C-terminal region. NT: N-terminal region.

Fluorescence Spectroscopic Studies. A 1.5 mL (0.1 mg/mL) aliquot of the HPLC-purified synthetic peptide mimicking eLP_2 of the TP receptor in constrained loop form or open form dissolved in 0.01 M phosphate buffer, pH 7.2, containing 0.1 M NaCl was incubated with 5 μL of ethanol containing 0−10.32 μM SQ29,548 or Iloprost. Fluorescence spectra were acquired with an SLM SPF500C spectrofluorometer with a built-in microprocessor at room temperature in a 1.0 cm path length nonfluorescence cell. Recorded spectrum data were downloaded to a PC computer for further analysis.

Circular Dichroism. The peptide in the constrained loop or open form was dissolved in 0.01 M phosphate buffer, pH 6.5, containing 0.1 M NaCl, at a concentration of 0.3 mg/mL. Different concentrations of SQ29,548 were dissolved in 10 μL of ethanol and then added to 3 mL of the peptide solution. For the peptide alone, only 10 μL of ethanol was added to normalize the concentration. Circular dichroism (CD) spectra were recorded with a JASCO-700 spectrometer, at room temperature, in a 1.0 cm path length cell.

NMR Sample Preparation. The HPLC-purified constrained loop peptide was dissolved in water and lyophilized 3 times to completely remove TFA and acetonitrile and then dissolved in 0.02 M sodium phosphate buffer, pH 6.0. The sample was lyophilized and rehydrated at a final concentration of 5 mM in H_2O containing 10% D_2O.

NMR Experiments. Proton NMR experiments were carried out on a VARIAN UNITY500 spectrometer. All 2D experiments (DQF-COSY, TOCSY, and NOESY) were performed under the same conditions (298 K in 20 mM, pH 6.0, sodium phosphate buffer containing 10% D_2O to provide a lock signal). The NOESY spectrum was recorded with a mixing time of 200 ms; the TOCSY spectrum was carried out with the DIPSI spin-lock sequence with a total mixing time of 50 ms. All spectra were composed of 2048 complex points in F2 and 512 complex points in F1 with 32 scans per t1

[1] Abbreviations: CD, circular dichroism; COSY, correlated spectroscopy; DPC, dodecylphosphocholine; DQF-COSY, double-quantum-filtered COSY; HPLC, high-pressure liquid chromatography; NMR, nuclear magnetic resonance; NOE, nuclear Overhauser effect; NOESY, nuclear Overhauser effect correlation spectroscopy; TOCSY, total correlation spectroscopy; 2D, two-dimensional.

increment. Quadrature detection was achieved in F1 by the states-TPPI method. The NMR data were processed using Felix 98. All FIDs were zero-filled to 2K-2K before Fourier transformation, and 0° (for DQF-COSY), 70° (for TOCSY), or 90° (for NOESY) shifted sinbell^2 window functions were used in both dimensions. The sequence-specific assignment was obtained using the standard method (*14*).

Calculation of Structures. The overall structure of the peptide was determined through the use of intraresidue, sequential, and long-range NOEs. NOE cross-peak volumes in the NOESY spectrum were converted into upper bounds of the interproton distances by using the Felix 98 program (Molecular Simulation, Inc., San Diego, CA). A total of 222 NOE cross-peaks were obtained and segmented using a statistical segmentation function and characterized as strong, medium, and weak, corresponding to upper bound distance range constraints of 2.5, 3.5, and 6.0 Å, respectively. By direct measurement of $^3J_{NH\alpha}$ values in the DQF-COSY spectrum, 17 of 21 dihedral angles were obtained. Distance geometry calculations were then carried out on an SGI workstation using the DGII program within Insight II package (Molecular Simulation, Inc.), and initial structures were calculated based on the NOE constraints and dihedral angles. The structures were further refined by restrained minimization and dynamic studies using the Discover program within the Insight II package.

Molecular Modeling of the TP Receptor. A 3D structural working model for the human TP receptor was constructed using homology modeling within the Insight II program based on the reference bacteriorhodopsin crystallographic structure (*8*, *15*). The sequence of human TP receptor was first searched from the Protein Data Bank (PDB) and aligned with the reference bacteriorhodopsin sequence. By copying the coordinates of structurally conserved transmembrane domains directly from the reference protein, the model of human TP receptor was first built with seven transmembrane helices (TMs). The loops that connect the TMs were generated by searching the database of known protein structures (*16*). The search criterion is the structural similarity of the conserved residues flanking the reference loop to those flanking the model loop in the database.

RESULTS

Characterization of the Interaction between Receptor Segment and Ligand. Synthetic receptor segments have been widely used to evaluate receptor−ligand interactions. Strong binding (with dissociation constants of 10^{-6}−10^{-8} M) of the synthetic acetylcholine receptor peptides to its ligand has been demonstrated by other studies (*17*). Using the same approach to test whether the synthetic loop peptides of the TP receptor are able to mimic the portion of the active receptor to interact with its ligand, the open and constrained loop forms of the peptides corresponding to the highly conserved eLP_2 were used to interact with SQ29,548, a TP receptor antagonist. The interaction was monitored by changes in the intrinsic fluorescence of a conserved Trp residue in the peptide. The fluorescence intensity of the constrained loop peptide was increased by addition of SQ29,-548 in a concentration-dependent fashion which saturated at about 5 μM concentration of the ligand (Figure 2). In contrast, no significant fluorescence changes were observed

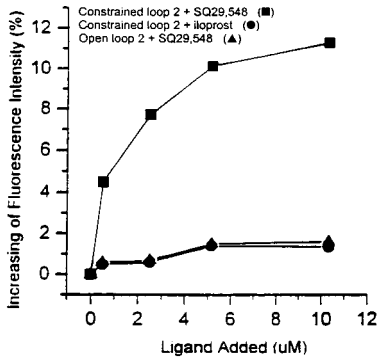

FIGURE 2: Fluorescence spectroscopic analysis for the interaction of the receptor ligand with the synthetic peptide corresponding to eLP2 of the TP receptor. The fluorescence spectra were recorded as described under Materials and Methods. The fluorescence enhancement of the synthetic peptide by addition of its ligand was plotted. The increase of the fluorescence intensity of the peptide was calculated by subtracting the fluorescence intensity obtained from the peptide in the absence of the ligand.

upon additions of Iloprost [a prostacyclin receptor (IP receptor) ligand] (Figure 2), PGD_2, or $PGF_{2\alpha}$ (data not shown) in the same concentrations of SQ29,548. The fluorescence changes were also not observed when SQ29,-548 was added to the open form peptide (Figure 2). These results indicated the changes in the environment of the Trp residue in the constrained loop peptide upon interaction with the specific TP receptor ligand and not with IP receptor ligand. It supports that the constrained loop peptide was able to mimic a portion of the functional receptor, and that eLP_2 of the TP receptor can be involved to form specific ligand recognition site(s). The results also suggest that the open form of the extracellular loop peptide has a different conformation compared to the constrained loop form.

CD Spectroscopy Analysis. CD spectroscopy was performed to further characterize the secondary structures of the peptides. As expected, the secondary structure of the constrained loop peptide was significantly changed by the addition of SQ29,548 (Figure 3A). However,, SQ29,548 has little effect on the open form peptide (Figure 3B). Iloprost also did not affect the CD spectra of the constrained loop peptide (Figure 3C). In addition, significantly different secondary structures were observed for the open and constrained loop forms of eLP_2 from the CD spectra. The constrained loop peptide has a higher content of β-sheet and turn structures, and less helical structure than the open peptide (Figure 3A,B). These results bring up very interesting further questions as to what residues of the constrained loop peptide make up the β-turn structure, and how the spacer connection of the N- and C-termini of the constrained loop peptide helps to stabilize the loop conformation. Determination of the 3D solution structure of the constrained eLP2 peptide was performed to address the questions.

NMR Assignment. 2D NMR spectra of the peptide were recorded in H_2O, and ^1H NMR assignments were accomplished using the standard sequential assignment technique. The procedure involves identification of spin systems and sequential assignment using a combination of TOCSY, DQF-COSY, and NOESY (data not shown) spectra recorded in H_2O. The complete proton resonance assignments for the peptide are summarized in Table 1. From the NOESY spectrum, 222 constraints were obtained, which included 102

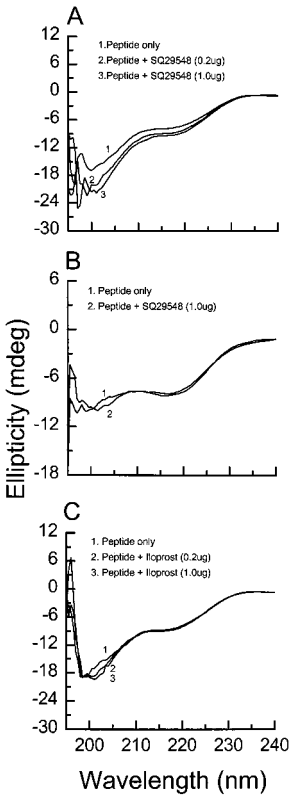

FIGURE 3: CD spectroscopic analysis for the interaction of eLP2 of the TP receptor with its ligand. The peptide in the constrained loop (A, C) and open (B) forms was recorded with a Jasco J-700 spectrometer at room temperature in a quartz optical cell with 0.1 cm path length in the absence or presence of ligand.

Table 1: Proton Chemical Shifts and Coupling Constants for TP Receptor eLP_2 Peptide

residues	HN	Hα	Hβ1	Hβ2	others	$^3J_{NH\alpha}$[a]
hCys1	8.23	4.29	1.91		2.38	M
Arg2	8.52	4.32	1.41		1.63, 3.04, 7.02	M
Tyr3	8.30	3.88	2.78	2.96	6.97	M
Thr4	8.11	4.31	4.08		1.05	M
Val5	7.98	3.96	1.89		0.79, 0.72	M
Gln6	8.15	4.17	1.76	2.07		M
Tyr7	7.91	4.23	2.72	2.9	6.93	overlap with Leu16
Pro8		4.00	2.44	2.56	2.14, 2.08	
Gly9	7.82	3.68			3.61	W
Ser10	7.99	4.25	3.76	3.67		M
Trp11	7.92	4.50	3.15		7.46, 9.99, 7.02	W
Cys12	7.77	4.26	2.52	2.63		M
Phe13	7.86	4.44	2.87	3.04	7.11	W
Leu14	8.06	4.22	1.51		0.76, 1.03	W
Thr15	7.84	4.24	4.11		1.09	S
Leu16	7.91	4.23	1.47		0.76	overlap with Tyr7
Gly17	8.14	4.31			3.79	M
Ala18	8.04	4.21	1.31			S
Glu19	8.18	4.25	1.89	2.05	2.34	S
Ser20	8.06	4.29	3.79	3.77		S
Gly21	8.37	4.10			3.86	W
Asp22	8.09	4.39	2.62	2.53		overlap with hCys23
hCys23	8.09	4.39	1.95		2.12	overlap with Asp22

[a] S, strong; M, medium; W, weak.

intraresidue, 71 sequential, and 49 long-range NOEs. The number of constraints per residue is shown in Figure 4. From the DQF-COSY spectrum, 17 well-defined and 4 overlapped dihedral angles were obtained (Table 1). Figure 5 shows the survey of the sequential and medium-range NOEs and the spin−spin coupling constants of the peptide, which show the potential two β-turn position of the peptide.

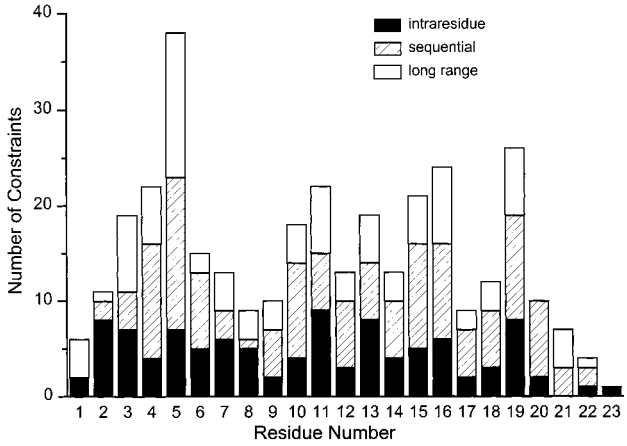

FIGURE 4: Number of constraints per residue for eLP2 of the TP receptor: intraresidue (filled bars), sequential (hatched bars), and long range (open bars).

Description of the 3D Structural Model of Human TP Receptor eLP2. On the basis of NOE constraints and dihedral angles, 8 of 100 first-generation structures with 2 rmsd (residues 5−19) were obtained using DGII program calculation (data not shown). The conformations show the trend of the two-turns loop. Energy refinement calculations (minimization/dynamic) were then carried out based on the best distance geometry structures using Discover program within Insight II, and 40 structures were obtained and superimposed as shown in Figure 6. The ordered NMR structures with 0.4 rmsd clearly show the two-turns conformations with the first turn at residue 9 and second turn at residue 14, which match the survey of the NOEs (Figure 5). The distance between N- and C-termini of eLP2 is 14.2 Å.

Configuration of the eLP_2 Structure on the TP Receptor Model. The NMR structure of the eLP_2 was grafted on the TP receptor working model constructed by homology modeling using the crystallographic structure of bacteriorhodopsin as template as described above. The configuration was based on the three following considerations: (1) connecting the N- and C-termini of the NMR structure of the eLP_2 into the C- and N-termini of the fourth (TM4) and fifth (TM5) transmembrane helices; (2) matching the 14.5 Å of the predicted distance between TM4 and TM5 in the working model with the determined N- and C-terminal distance of the eLP_2 with 14.2 Å; and (3) forming a disulfide bond between residue 105 in the beginning of the extracellular loop 1 and residue 183 in eLP_2, which has been demonstrated by site-directed mutagenesis studies described previously (*10*, Figure 7). After the configuration, 500 steps of energy minimization were used to refine the conformation of the eLP2 in the predicted working model. As showed in Figure 7, the determined eLP2 peptide could be perfectly fixed into the conserved transmembrane domains 4 and 5 with respect to the cysteine disulfide bond.

DISCUSSION

A conformational change in the constrained eLP2 of the TP receptor was detected by fluorescence spectroscopy upon interaction with SQ29,548 (Figure 2). These studies offer one of the methods to identify binding sites of peptides corresponding to other portions of the extracellular domains. There are Trp residues in the N-terminal domain and first

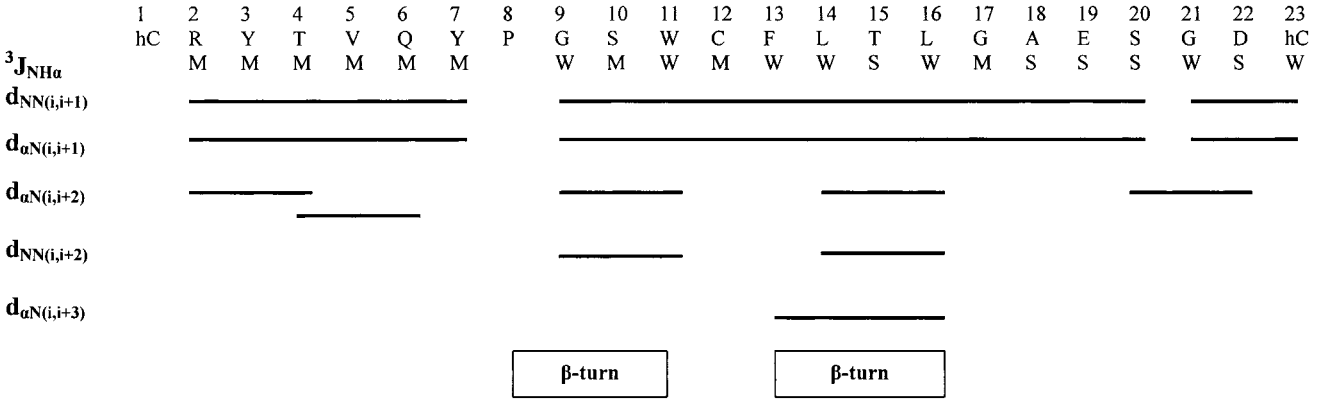

FIGURE 5: Amino acid sequence of TP receptor eLP2 and a survey of sequential and medium-range NOEs, HN−Hα coupling constants of the peptide. The values of the $^3J_{NH\alpha}$ coupling constants are reported in the notations of S (strong), M (medium), and W (weak). At the bottom of the figure, the locations of turn structures are shown.

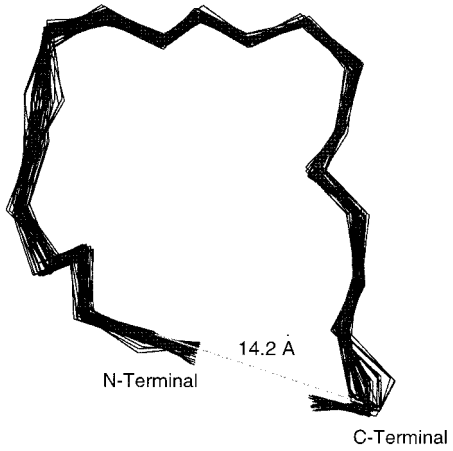

FIGURE 6: Superimposition of the best 40 structures using just the α-carbons obtained from energy refinement calculations. The distance between the N-terminal and the C-terminal (residues 2 and 22) is 14.2 Å.

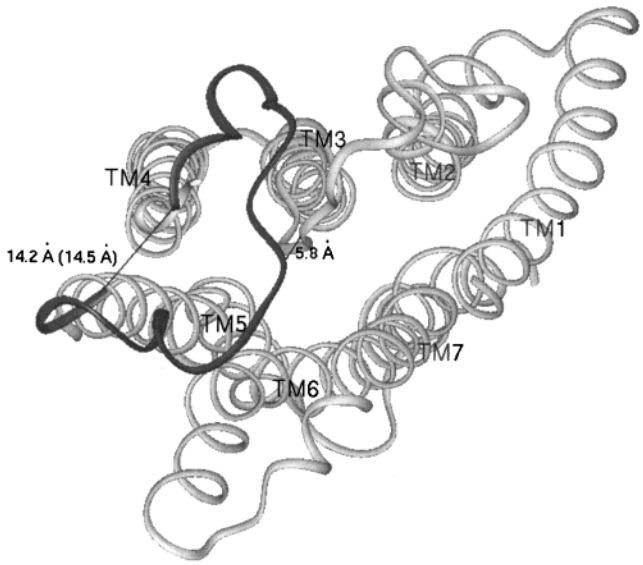

FIGURE 7: TP receptor model generated from molecular modeling based on the bacteriorhodopsin crystallographic structure, with transmembrane helices 1−7 (TM1−TM7, light lines). The NMR structure of eLP2 (dark line) of the TP receptor was connected to TM4 and TM5. The distance from the TP receptor model between helices 4 and 5 was 14.5 Å. The distance from the NMR structure of TP receptor eLP2 was 14.2 Å.

extracellular loop of the TP receptor which generate an intrinsic fluorescence signal for these peptides. The method described above for the eLP2 studies can be adopted for these peptide studies. As described above, the CD studies were able to detect the significant secondary structural changes of the constrained eLP2 upon ligand binding. The same approach can be used to characterize ligand binding to other peptides corresponding to the N-terminal domain, and the first and third extracellular loops of the TP receptor to identify whether the open or the constrained loop forms of the first and third extracellular loop peptides bind the specific ligand. It should be indicated that we are still working on the studies of the interaction between the eLP2 peptide and SQ29,548 using NMR experiments. However, we had difficulty obtaining a reasonable concentration of SQ29,-548 in water for the experiments so far.

3D structures are not yet available for mammalian G protein-coupled receptors, due in large part to the difficulties in crystallizing membrane-bound proteins. Little information also is available about the structural basis of the ligand-specific recognition with the extracellular parts of the prostanoid receptors. All members of the G protein-coupled receptor superfamily are believed to adopt the same basic structure in the membrane-embedded regions because of their sequence similarities and their common function of interaction with G proteins (*18*). Several 3D structural models of mammalian G protein receptors (*19*−*22*) have been constructed using molecular modeling based on bacteriorhodopsin crystal structures (*23*−*25*); especially, a high resolution structure of bacteriorhodopsin has been solved recently (*26*). Our initial working model for the human TP receptor (Figure 1), constructed by molecular modeling based on the bacteriorhodopsin structure, was used to guide our experimental designs. The approach may be suitable for the studies of structural and functional relationship of other prostanoid receptors.

Synthetic peptides have emerged as important tools in characterizing the functional domains of several receptors including G protein-linked receptors (*27*−*31*). Peptides corresponding to the C-terminal extramembranous domains of the angiotensin II AT1A receptor (*27*), natriuretic peptide receptor C (*28*), and testicular follicle stimulating hormone receptor (*30*) had functional activities indicating that the peptides can adopt the native structures in the cognate parts of the intact receptors. Peptides with sequences corresponding to the extramembranous loops and the C-terminal tail of

bovine rhodopsin have been confirmed to have biological activity (*32*, *33*), and, importantly, the individual peptides were found to form defined loops or globular structures in solution as determined by 2D NMR techniques recently (*34*−*38*). The findings were further supported by using the spin-label technique on intact membrane-bound rhodopsin in which the specific site-to-site distances measured on the intact protein agreed with the spacing on the peptide structures solved by the 2D NMR technique (*39*, *40*). These successful studies are consistent with our finding in the determination of the extracellular domains for the TP receptor in the studies. Results from our studies are important for understanding the structure/function relationship of the human TP receptor, and will also provide evidence to solve the solution 3D structures of these important domains of other prostanoid receptors and other G protein-coupled receptors.

ACKNOWLEDGMENT

We thank Dr. Xiaolian Gao in the Chemistry Department, University of Houston, for access to the NMR facility and providing valuable advice on taking the NMR spectra. Acknowledgment is also made to the Robert A. Welch Foundation and the W. M. Keck Center for Computational Biology at the University of Houston for computer resource support.

REFERENCES

1. Majerus, P. W. (1983) *J. Clin. Invest. 72*, 1521−1525.
2. Miller, D. K., Sadowski, S., Soderman, D. D., and Kuehl, F. A., Jr. (1985) *J. Biol. Chem. 260*, 1006−1014.
3. Negishi, M., Sugimoto, Y., and Ichikawa, A. (1995) *Biochim. Biophys. Acta 1259*, 109−120.
4. Coleman, R. A., Kennedy, I., Humphrey, P. P. A., Bunce, K., and Kumley, P. (1990) *Prostanoid and their receptor in Comprensive Medicinal Chemistry* (Hansch, C., Sammes, P. G., Taylor, J. B., and Emmett, J. C., Eds.) Vol. 3, pp 643−714, Pergamon Press, Oxford.
5. Ushikubi, F., Nakajima, M., Hirata, M., Okuma, M., Fujiwara, M., and Narumiya, S. (1989) *J. Biol. Chem. 264*, 16496−16501.
6. Hirata, M., Hayashi, Y., Ushikubi, F., Yokata, Y., Kageyama, R., Nakanishi, S., and Narumiya, S. (1991) *Nature 349*, 617−620.
7. Raychowdhury, M. K., Yukawa, M., Collins, L. J., McGrail, S. H., Kent, K. C., and Ware, J. A. (1994) *J. Biol. Chem. 269*, 19256−19261.
8. Funk, C. D., Furci, L., Moran, N., and Fitzgerald, G. A. (1993) *Mol. Pharmacol. 44*, 934−939.
9. D'Angelo, D. D., Eubank, J. J., Davis, M. G., and Dorn, G. W., II (1996) *J. Biol. Chem. 271*, 6233−6240.
10. Chiang, N., Kan, W. M. J., and Tai, H.-H. (1996) *Arch. Biochem. Biophys. 334*, 9−17.
11. Dom, G. W., II, Davis, M. G., and D'Angelo, D. D. (1997) *J. Biol. Chem. 272*, 12399−12405.
12. Kobayashi, T., Kiriyama, M., Hirata, T., Hirata, M., Ushikubi, F., and Narumiya, S. (1997) *J. Biol. Chem. 272* (24), 15154−15160.
13. Audoly, L., and Breyer, R. M. (1997) *J. Biol. Chem. 272*, 13475−13478.
14. Wüthrich, K. (1986) *NMR of Proteins and Nucleic Acids*, John Wiley & Sons, New York.
15. Funk, C. D., Furci, L., FitzGerald, G. A., Grygorczyk, R., Rochette, C., Bayne, M. A., Abramovitz, M., Adam, M., and Metters, K. M. (1993) *J. Biol. Chem. 268*, 26767−26772.
16. Ruan, K.-H., Milfeld, K., Kulmacz, R. J., and Wu, K. K. (1994) *Protein Eng. 7*, 1345−1351.
17. Ruan, K.-H., Spurlina, J., Quiocho, F., and Atassi, M. Z. (1990) *Proc. Natl. Acad. Sci. U.S.A. 87*, 6156−6160.
18. Baldwin, J. M. (1993) *EMBO J. 12*, 1693−1703.
19. Tang, Y., Chjen, K. X., Jiang, H. L., Jin, G. Z., and Ji, R. Y. (1996) *Acta Pharmacol. Sin. 17*, 8−12.
20. Neumuller, M., and Jahnig, F. (1996) *Proteins: Struct., Funct., Genet. 26*, 145−156.
21. Wetzel, J. M., Salon, J. A., Tamm, J. A., Forray, C., Craig, D., Nakanishl, H., Cui, W., Vaysse, P. J., Chiu, G., Weinshank, R. L., Hartig, P. R., Branchek, T. A., and Gluchowski, C. (1996) *Receptors Channels 4*, 165−177.
22. Pogozheva, I. D., Lomize, A. L., and Mosberg, H. I. (1997) *Biophys. J. 72*, 1963−1985.
23. Henderson, R. (1975) *J. Mol. Biol. 93*, 123−138.
24. Henderson, R., Baldwin, J. M., Ceska, T. A., Zemlin, F., Beckmann, E., and Downing, K. H. (1990) *J. Mol. Biol. 213*, 899−929.
25. Grigorieff, N., Ceska, T. A., Downing, K. H., Baldwin, J. M., and Henderson, R. (1996) *J. Mol. Biol. 259*, 393−421.
26. Pebay-Peyroula, E., Rummell, G., Rosenbusch, J. P., and Landau, E. M. (1997) *Science 277*, 1676−1681.
27. Franzoni, L., Nicastro, G., Pertinhez, T. A., Tato, M., Nakaie, C. R., Paiva, A. C. M., Schreiner, S., and Spisni, A. (1997) *J. Biol. Chem. 272*, 9734−9741.
28. Anand-Srivastava, M. B., Sehl, P. D., and Lowe, D. G. (1996) *J. Biol. Chem. 271*, 19324−19329.
29. Grasso, P., Leng, N., and Reichert, L. E., Jr. (1995) *Mol. Cell. Endocrinol. 108*, 43−50.
30. Dias, J. A. (1996) *Mol. Cell. Endocrinol. 125*, 45−54.
31. Koke, H. K., Liotta, A. S., Kole, S., Roth, J., Montrose-Rafizadeh, C., and Bernier, M. (1996) *J. Biol. Chem. 271* (49), 31619−31626.
32. Takemoto, D. J., Morrison, D., Davis, L. C., and Takemoto, L. J. (1986) *Biochem. J. 235*, 309−312.
33. Konig, B., Arendt, A., McDowell, J. H., Kahlert, M., Hargrave, P. A., and Hofmann, K. P. (1989) *Proc. Natl. Acad. Sci. U.S.A. 86*, 6878−6822.
34. Yeagle, P. L., Aiderfer, J. L., and Albert, A. D. (1995a) *Nat. Struct. Biol. 2*, 832−834.
35. Yeagle, P. L., Alderfer, J. L., and Albert, A. D. (1995b) *Biochemistry 34*, 14621−14625.
36. Yeagle, P. L., Alderfer, J. L., and Albert, A. D. (1996) *Mol. Vision 2* (http: www.emory.edu/molvis/v2/yeagle).
37. Yeagle, P. L., Alderfer, J. L., Salloum, A. C., Ali, L., and Albert, A. D. (1997) *Biochemistry 36*, 3864−3869.
38. Yeagle, P. L., Alderfer, J. L., and Albert, A. D. (1997) *Biochemistry 36*, 9649−9654.
39. Farrens, D. L., Altenbach, C., Yang, K., Hubbell, W. L., and Khorana, H. G. (1996) *Science 274*, 768−770.
40. Yang, K., Farrens, D. L., Altenbach, C., Farahbakhsh, Z. T., Hubbell, W. L., and Khorana, H. G. (1996) *Biochemistry 35*, 14040−14046.

BI001867C